Second Conference on Smart Monitoring,
Assessment and Rehabilitation of Civil Structures

SMAR 2013

Cyclic testing of a steel-core buckling restrained brace under near-fault displacement reversals

C. Avci Karatas[1], S. Cetinkaya[1], C. Demir[2], B. Gunes[3], M. Comert[2], and O. C. Celik[4]

[1] Institute of Science and Technology, Istanbul Technical University, Istanbul, Turkey
[2] Department of Civil Engineering, Civil Engineering Faculty, Istanbul Technical University, Istanbul, Turkey
[3] Department of Civil Engineering, Engineering Faculty, Istanbul University, Istanbul, Turkey
[4] Division of Theory of Structures, Faculty of Architecture, Istanbul Technical University, Istanbul, Turkey

ABSTRACT: Buckling Restrained Braces (BRBs), display a balanced hysteretic behavior by axial yielding under reversed cyclic tension and compression forces. Although component testing of BRBs is conducted under various symmetrical cyclic displacement loading protocols, the use of unsymmetrical protocols in testing to account for near-fault effects of ground shaking are quite limited. To investigate the performance under such a loading, one full scale steel-core BRB specimen (named as TURKBRACE BRB-SC1) with simple details has been designed to AISC specification, fabricated, and cyclically tested. TURKBRACE BRB-SC1 exhibited excellent performance under fatigue and near-fault loading histories. Experimental results show that the BRB specimen reached a maximum drift of 6%, while no fractures in the welds or any sign of local or global instability were observed. Hysteretic curves, behavioral values such as maximum strength in tension and compression cycles, stiffness changes with displacement cycles, hysteretic damping, and cumulative hysteretic energy dissipation values are given.

1 INTRODUCTION

Special considerations may be required for structures equipped with buckling restrained braces (BRBs) located in near-fault regions. Unsymmetrical protocols to account for near-fault effects of earthquakes are quite limited. Experimental and numerical studies have been conducted to promote the application of different types of BRBs. Takeuchi et al. (2008, 2012) proposed a simple method for predicting the cumulative deformation and energy absorption capacities of BRBs under random amplitudes. Vargas and Bruneau (2009a, 2009b) proposed an alternative design approach for systems with metallic fuses. An experimental work was also conducted on a three-story frame designed with BRBs to verify the proposed design procedure. A series of performance tests and analyses were carried out by Usami et al. (2009) to clarify the requirements of high-performance BRBs for the damage controlled seismic design of steel bridges. To increase the efficiency of buckling restrained braced frames (BRBFs), a novel connection where the gusset is only connected to the beam and is offset from the column face was proposed and tested in a three-story frame under quasi-static loading by Berman and Bruneau (2009). Celik and Bruneau (2009, 2011) analytically investigated the best geometrical layout to maximize the dissipated hysteretic energy in ductile diaphragms with BRBs end diaphragms in straight and skewed steel bridges. Component tests were conducted by Zhao et al. (2012) to address the effect of brace end rotation on the global buckling behavior of pin-connected BRBs with end collars. Mostly, the concepts of BRBs published or applied for patents are essentially similar and the BRB's core brace member is mostly manufactured of steel owing to its great hysteretic performance. As an alternative to commercially available BRB types, produced under the patent of various firms in the U.S.A and Japan, a total of 8 BRBs (4 as preliminary studies, 2 with steel core and outer tube, 2 with aluminum alloy core and outer tube) having the same yield strength and simple end connection details are designed, produced, and tested (Karatas and Celik 2011, 2012, Karatas 2012). Examining the possible superiorities of steel core BRBs that are developed herein is considered to be of importance in terms of earthquake engineering research and design applications. Although component testing of BRBs is conducted under various symmetrical cyclic displacement loading protocols, the use of unsymmetrical protocols in testing to account for near-fault effects of ground shaking are quite limited (Tsai and Lai 2002, Ookouch et al. 2006). To investigate the performance under such a loading, one full scale steel-core BRB specimen (named as TURKBRACE BRB-SC1) with simple details has been designed to AISC specification, fabricated, and cyclically tested in the Structural and Earthquake Engineering Laboratory (STEEL) of the Technical University of Istanbul. The specimen is well-instrumented to gather significant data during testing. Details of the test set-up, specimens, cyclic testing of specimens, experimental observations, and conclusions are summarized in this work.

2 EXPERIMENTAL PROGRAM

2.1 Test set-up and instrumentation

A versatile test set-up composed of a steel L frame, previously constructed for cyclic testing of classical (i.e. buckling) braces and designed to accommodate different bracing sizes and lengths (Figure 1a, Haydaroglu et al. 2011), is modified and used in this work. The test set-up was designed to remain elastic under the maximum actuator force. The steel grade used for testing set-up was S275JR. Loads were applied by a computer-controlled MTS hydraulic actuator, capable of producing up to 250kN horizontal loading. Displacement (or stroke) capacity of the actuator is ±300mm. Displacement controlled testing was carried out via double LVDTs mounted on the column face at the same height with the actuator. The specimen was designed well less than the capacity of the actuator. The specimen was tested at a 38-degree diagonal bracing configuration with the steel foundation beam. Cyclic responses of the column, foundation beam, and BRBs were obtained from the strain gauges and LVDTs installed at critical points. In total, 21 strain-gauges were installed on TURKBRACE BRB-SC1 and testing set-up (Figure 1b).

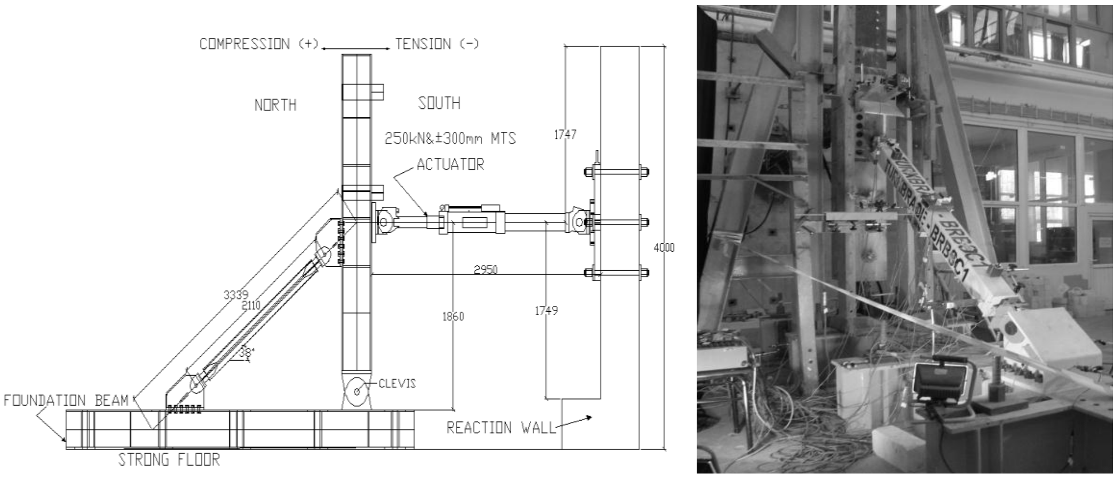

(a) (b)

Figure 1. Test set-up (a) general view (b) instrumentation for specimen.

2.2 Material characteristics

Three tensile test specimens (coupons) were prepared in prototype samples according to the recommended standard (ASTM-A370-08a, 2008). TURKBRACE BRB-SC1 was made of S235JR normal strength steel. Prior to testing, these material data were used in static pushover analyses of the specimens, using SAP2000 v14 (CSI 2009) to predict the load-displacement curves of the specimens. The average coupon test results of the specimen are listed in Table 1. Here, ε_y, ε_u, F_{ysc}, F_u, E are yield strain, total tensile strain at fracture, yield strength/stress, ultimate tensile strength, and modulus of elasticity, respectively. Compression tests of the infill/mortar material revealed that the specified 7-day and 28-day mortar strengths were 52.3MPa and 64.1MPa, respectively. Steel bolts used are fully-tensioned, high-strength A490Grade (10.9) in gussets-to-BRB and gussets-to-L frame connections. Specially designed gusset-plates were used for the BRB to avoid out-of-plane buckling.

Table 1. Average material properties of steel core

TURKBRACE BRB-SC1	ε_y (%)	ε_u (%)	F_{ysc} (MPa)	F_u (MPa)	E (GPa)
S235JR	0.15	38.21	257	363	195

2.3 Details of specimens

The specimen uses single bolted (pinned) end connections and a rectangular shaped core plate (16mmx30mm) made of S235JR steel which expands at the ends to form a cruciform section. The core is surrounded by a steel square outer tube infilled with a high strength grout as buckling restraining system. General views from the end connection and elevation of BRB are given in Figure 2a,2b. The geometrical parameters are summarized in Table 2. The length and width of the yielding portion of the brace are denoted by L_{ysc} and b_{ysc}, respectively. Likewise, L_{con} and b_{con}, are the length and width of the connection portion. The transition zone has a length of L_{tr} and a width of b_{tr}. t denotes the thickness of the core. Total length of the BRB is limited to 2275mm. It is clear that the restraining member of the BRB does not intend to withstand any axial force. P_e/P_{ysc}, ratio of the Euler buckling load of the outer tube (P_e) to the yield load of the core (P_{ysc}), has to be checked as a criterion to guarantee the yielding of the core material. Watanabe et al. (1988) suggested that this ratio (P_e/P_{ysc}) should be over 1.5, a higher ratio of 30.9 was used in this work for TURKBRACE BRB-SC1. A key issue of the design is to ensure a proper sliding between the core and mortar to avoid relevant shear stress transfer. In the proposed BRB, this is ensured by a three-layer interface. The steel core is coated with Polytetrafluoroethylene as the unbonding material.

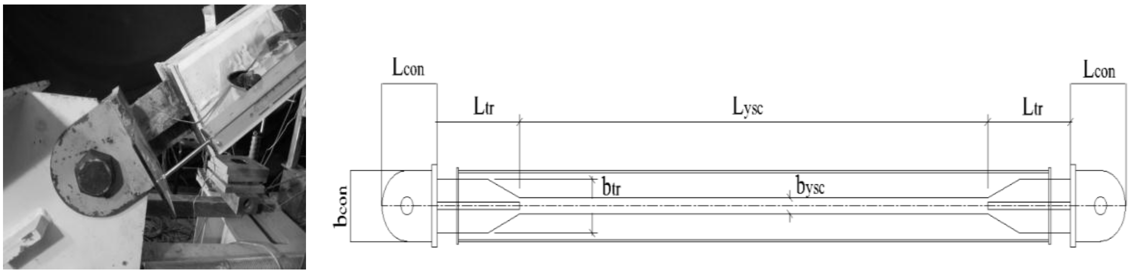

(a) (b)

Figure 2. Specimen details, (a) General views from the end connection, (b) Elevation.

Table 2. General geometrical parameters of the steel core

Specimen	L_{ysc} (mm)	b_{ysc} (mm)	t (mm)	L_{con} (mm)	b_{con} (mm)	L_{tr} (mm)	b_{tr} (mm)
TURKBRACE BRB-SC1	1410	30	16	185	165	249	100

According to AISC-341 (2010), the axial yield strength of the BRB, P_{ysc}, shall be determined by Eq.(1):

$$P_{ysc} = \beta\omega R_y F_{ysc} A_{sc} \tag{1}$$

where β and ω are the compression and strain-hardening adjustment factors, respectively, R_y is the ratio of the expected yield stress to the specified minimum yield stress, F_{ysc} is the specified actual yield stress of the core as determined from the coupon test, and A_{sc} is the net area of the core. The ω factor is calculated as the ratio of the maximum tension force (T_{max}) measured from the qualification tests to the yield force, P_{ysc}, of the test specimen. The β factor is calculated as ratio of the maximum compression force (P_{max}) to the maximum tension force. Numerical values of β and ω at the point of maximum deformation were obtained from previous studies (e.g., Meritt et al. 2003, and Lopez and Sabelli, 2004) as 1.15 and 1.45. Further details regarding the specimen can be found in Karatas and Celik (2012), and Karatas (2012).

3 TESTING

3.1 Loading protocol

In the present study, the testing employed two cyclic testing patterns. Firstly, a low-cycle fatigue loading protocol to achieve a cumulative inelastic axial deformation, η of at least $200\Delta_{by}$ (AISC-341, 2010) (Δ_{by}= first axial yielding deformation of BRB) has been run before the application of the near-fault loading protocol used by Uang et al. (2000). Top horizontal displacement is related to the brace axial displacement and was taken as the displacement control parameter. Δ_{by}, was estimated as 5.41mm in static pushover analyses of the specimen, conducted using SAP2000 v14 and was used to initially control the test. However, the experimentally obtained values were used as test control parameters beyond the elastic range. This was determined at the onset of visible nonlinearity in the force-displacement curve, or by using the strain-gauge data that was obtained in the mid-section of steel core.

The loading history was begun with 2 cycles of the loading at the elastic displacement corresponding to $1/4\Delta_{by}$, $2/4\Delta_{by}$, and $3/4\Delta_{by}$, sequentially. The first testing pattern was conducted with amplitude of $\pm 2.03\Delta_{by}$ until 96 cycles of %0.65 drift. At the end of low-cycle-fatigue protocol, η was achieved as $201.76\Delta_{by}$. Once the low-cycle-fatigue loading protocol was completed for the specimen, near-fault loading protocol (developed by Krawinkler, 1996) was used (Figure 3a). The sequence begins with a push (compression) to -2% drift (-12.00mm), followed by a large pull (tension) up to a +6% drift (+111.60mm). There are then cycles between +1% (+18.60mm) and +5% (+93.00mm) drift, narrowing to cycles between +2% (+37.20mm) and +4% (+74.40mm) drifts, and again up to +6% drift. The sequence then pushes across zero to -2% drift, back up to +3% drift (+55.80mm), and back down to -1% drift (-8.50mm). Finally, there are several cycles between +3% and 0% drift, narrowing to between +2% and 0% drift (Figure 3b).

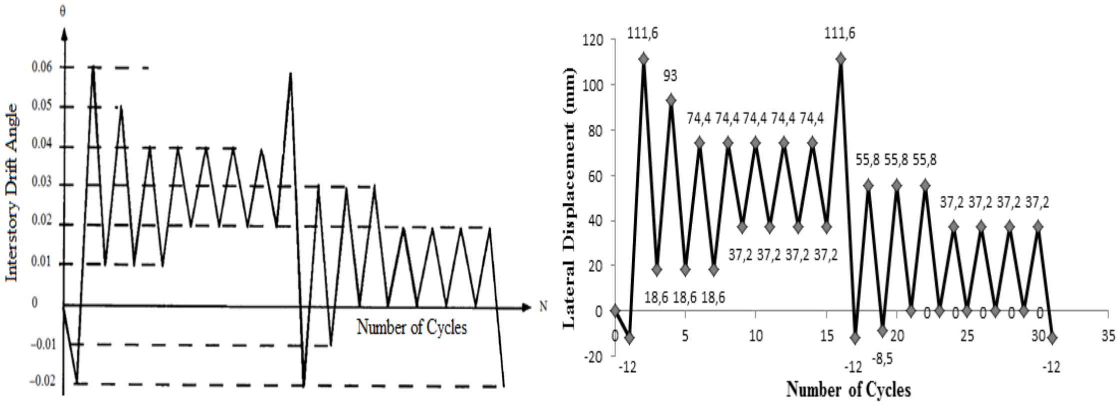

(a) (b)

Figure 3. Near-fault loading protocol used for TURKBRACE BRB-SC1 (a) In terms of interstory drift angle (b) In terms of lateral displacements.

4 EXPERIMENTAL OBSERVATIONS

Figure 4a shows TURKBRACE BRB-SC1 installed in the test set-up and ready for testing. Two gusset-plates are placed at both ends to ensure a proper anchoring to the test set-up. Loading protocol was rearranged since the actuator's capacity would have been exceeded during compression loadings. According to the low-cycle-fatigue loading protocol, the number of cycles which will enable the cumulative inelastic axial deformation (η) for the specimen to be $200\Delta_{by}$ at levels of $\pm2.03\Delta_{by}$ and ±12.00mm lateral displacement (0.65% drift), was found as 96. After 96 cycles, η was calculated as $201.76\Delta_{by}$. η value at the end of near-fault loading protocol was $381.56\Delta_{by}$. General views from the axial displacements at upper end of brace at +6% and -2% drifts are given in Figure 4b and 4c, respectively. No fracture in steel core, brace instability or no brace-to-end connection failures of any kind were observed in TURKBRACE BRB-SC1. Using experimental hysteresis, some behavioral characteristics of the specimens such as maximum strengths in tension and compression cycles, η cumulative inelastic deformation, E_h cumulative hysteretic energy dissipation, and ξ_{effb} equivalent damping ratio value are summarized. Experimental horizontal force-horizontal displacement hysteretic curve representing the cyclic behavior for specimen is given in Figure 5a. Out-of-plane displacement hysteretic curve is depicted in Figure 5b. Out-of-plane displacement of mid-span of the specimen's outer tube was measured between -0.18mm~+0.44mm. These values prove that out-of-plane buckling was effectively prevented during testing.

(a) (b) (c)

Figure 4. Images during testing (a) Overall view from the specimen prior to testing, (b) Axial displacement of upper end of brace at +6% drift, (c) Axial displacement of upper end of brace at -2% drift.

The experimental value of Δ_{by} was obtained as 5.91mm. Also, the reached maximum tension (T_{max}) and compression capacities (P_{max}), ω, β by the first cycle at $\pm\Delta_{by}$ (0.32% drift) were +98.62kN, -165.90kN, 0.78, and 1.68, respectively.

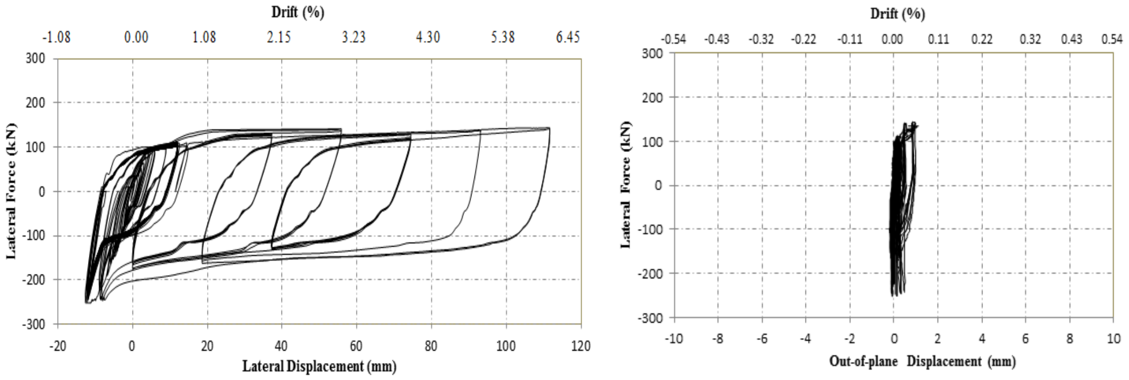

(a) (b)

Figure 5. Experimental hysteretic curves for specimen, (a) Lateral force vs. lateral displacement, (b) Lateral force vs. out-of-plane displacement.

5 DISSIPATED HYSTERETIC ENERGY AND EQUIVALENT DAMPING RATIO

For any cycle, total area under experimentally obtained hysteretic curve gives the dissipated energy through inelastic behavior. Since the cumulative energy dissipation is a useful measure of the seismic efficiency of a structural system, these values were calculated and the variation of cumulative energy dissipation with cumulative number of cycles is plotted in Figure 6. Numerical values of the cumulative hysteretic energy E_h and cumulative inelastic deformation η achieved by the specimen are 464508.50kN.mm and 381.56Δ_{by}, respectively. The most common method for defining equivalent damping ratio is to equate the energy dissipated in a cycle of the brace (Chopra, 2001). The computed value of equivalent damping ratio, ξ_{effb}, was obtained 45.08% for TURKBRACE BRB-SC1. Maximum value of ξ_{effb} is taken as a representative value of equivalent damping. Since ξ_{effb} for the specimen is greater than 15%, the tested steel BRB can be classified as an Energy Dissipating Device (EDD) as per EN 15129 D.1 (2010).

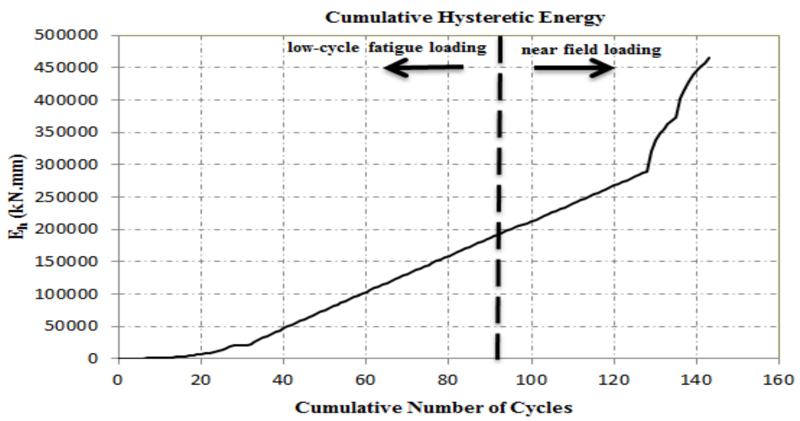

Figure 6. Cumulative energy dissipation.

6 CONCLUSIONS

TURKBRACE BRB-SC1 exhibited excellent performance (without buckling or fracture) under the fatigue and near-fault loading histories. Based on the test results presented herein, the following conclusions and observations can be drawn from this work:

- Experimental results show that the BRB specimen reached a maximum drift of 6% that corresponds to 111.60mm, while no fractures in the welds or any sign of local or global instability were observed.
- The maximum cumulative inelastic deformation is calculated as $381.56\Delta_{by}$, which satisfies the requirement of $200\Delta_{by}$ as proposed by AISC-341 (2010).
- Examinations on the damaged BRB demonstrate that the interior reserve gap, required to prevent bearing between core and mortar, formed within the specimen and thickness of unbonding material is required to be increased. With the information gained from this test, details of the interior reserve gap are improved for the forthcoming experiments.
- Hysteretic curves, behavioral values such as maximum strength in tension and compression cycles, stiffness changes with displacement cycles, hysteretic damping, and cumulative hysteretic energy dissipation values are given for near-fault loading protocol. An equivalent damping ratio of 45.08% is obtained during testing.

As a result, the BRB with unique details developed in this work showed promise for use in buildings that lack strength, stiffness, ductility, and located in near-fault regions.

7 ACKNOWLEDGMENTS

This research was supported in part by the Scientific and Technological Research Council of Turkey (TUBITAK) and the Istanbul Technical University Research Projects Unit (ITU-BAP). Steel gusset plates and bolts were produced by CIMTAS. Unbonded material was provided by FIBERFLON. High strength grout was provided by KOSTER. Technical assistance from the staff at Istanbul Technical University, Structural and Earthquake Engineering Laboratory (ITU-STEEL) and Bogazici University, Civil Engineering Department, Structures Laboratory are gratefully acknowledged and appreciated. However, any opinions, findings, conclusions, and recommendations presented in this paper are those of the authors and do not necessarily reflect the views of the sponsors.

8 REFERENCES

AISC. 2010. ANSI/AISC 341-10 Seismic Provisions for Structural Steel Buildings. *American Institute of Steel Construction*, Inc., Chicago.

ASTM A370-08a. 2008. Standard test methods and definitions for mechanical testing of steel products. *ASTM International*, 100 Barr-Harbor Drive, PO Box C700, Wast Conshohocken, PA 19428-2959.

Berman, J and Bruneau, M. 2009. Cyclic testing of a buckling restrained braced frame with unconstrained gusset connections. *ASCE Journal of Structural Engineering*, *ASCE*, Vol.135, No.12, pp.1499-1510.

Celik, OC and Bruneau, M. 2009. Seismic behavior of bidirectional-resistant ductile end diaphragms with buckling restrained braces in straight steel bridges. *Engineering Structures Journal*, Vol.31, Issue 2, February, pp.380-393.

Celik, OC and Bruneau, M. 2011. Skewed slab-on-girder steel bridge superstructures with bidirectional-ductile end diaphragms. *Journal of Bridge Engineering*, ASCE, Vol.16, No.2, March, pp.207-218.

Chopra, AK. 2001. *Dynamics of structures, theory and applications of earthquake engineering. 2nd Edition*. Prentice-Hall, Chapter 3, Response to harmonic and periodic excitations.

EN 15129 D.1. 2010. Anti-seismic devices. *European Committee for Standardization (CEN/TC 340)*.

Haydaroglu, C, Taskin, K, and Celik, OC. 2011. Ductility enhancement of round HSS braces using CFRP sheet wraps. *EUROSTEEL 2011*, August 31- September 2, Budapest, Hungary.

Karatas, Avci, C and Celik, OC. 2011. Design and fabrication of aluminum alloy core buckling restrained braces (BRBs). *Proceedings of the 4th Steel Structures Symposium*, Turkish Chamber of Civil Engineers (TMMOB), October 8-9-10, Istanbul, Turkey (in Turkish).

Karatas, Avci, C and Celik, OC. 2012. Experimental and numerical investigation of hysteretic behaviors of buckling restrained braces (BRBs) having steel and aluminum alloy cores. *Technical Report*, No.110M779, TUBITAK-MAG, Ankara, Turkey.

Karatas, Avci, C. 2012. Design, fabrication, and cyclic behavior of steel and aluminum alloy core buckling restrained braces (BRBs). *PhD Thesis*, Istanbul Technical University, Istanbul, Turkey.

Krawinkler, H. 1996. Cyclic loading histories for seismic experimentation on structural components. *Earthquake Spectra, The Professional Journal of the Earthquake Engineering Research Institute*, Vol. 12, Number 1, pp. 1-12.

Lopez, WA and Sabelli, R. 2004. Seismic design of steel buckling-restrained braced frames. *Steel Tips*, Structural Steel Education Council Technical Information & Product Service, July.

Meritt, S, Uang, CM, and Benzoni, G. 2003. Subassemblage testing of Star Seismic buckling restrained braces. *Technical Report*, No. TR-2003/04, Department of Structural Engineering, University of California, San Diego.

Ookouch, Y, Takeuchi, T, Uchiyama, T, Suzuki, K, Sugiyama, T, Ogawa, T, and Kato, S. 2006. Experimental studies of tower structures with hysteretic dampers. *Journal of the International Association for Shell and Spatial Structures: IASS*, Vol. 47, No.3, December n.152.

SAP2000 v14. 2009. Structural Analysis Program. *Computers and Structures Inc*.

Takeuchi, T, Ida, M, Yamada, S, and Suzuki, K. 2008. Estimation of cumulative deformation capacity of buckling restrained braces. *Journal of Structural Engineering*, *ASCE*, Vol.134, No.5,May 1, pp.822-831.

Takeuchi, T, Matsui, R, Tada, T, and Nishimoto, K. 2012. Out-of-plane stability of buckling restrained braces including their connections. *15th World Conference on Earthquake Engineering*, 24-28 September, Lisbon, Portugal.

Tsai, KC and Lai, JW. 2002. A study of buckling restrained seismic braced frame, *Structural Engineering*, 17(2) 3–32.

Uang CM, Yu QS, Gilton, CS. 2000. Effects of loading history on cyclic performance of steel RBS moment connections. *Proceedings of the 12th WCEE*, Upper Hutt, New Zealand, 2000.

Usami, T, Ge, H, and Luo, XQ. 2009. Experimental and analytical study on high-performance buckling restrained brace dampers for bridge engineering. *3rd International Conference on Advances in Experimental Structural Engineering*, October 15-16, San Francisco.

Vargas, RE and Bruneau, M. 2009a. Experimental response and design of buildings with metallic structural fuses II. *Journal of Structural Engineering*, ASCE, April 2009/395, Vol.135, No.4, pp.394-403.

Vargas, RE and Bruneau, M. 2009b. Analytical response and design of buildings with metallic structural fuses I. *Journal of Structural Engineering*, ASCE, April 2009/387, Vol.135, No.4,pp.386-393.

Watanabe, A, Hitomi, Y, Saeki, E, Wada, A, and Fujimoto, M. 1988. Properties of brace encased in buckling-restraining concrete and steel tube. *Proceedings of 9th World Conference on Earthquake Engineering*, Tokyo-Kyoto, Japan.

Zhao, J, Wu, B, and Ou, J. 2012. Effect of the brace end rotation on the global buckling behavior of pin-connected buckling-restrained braces with end collars. *Engineering Structures Journal*, Vol.40, pp.240-253.